

Supporting Information

3D Nanostructured Conductive PANI/MXene Hydrogels for Durable Aqueous Zn-ion Batteries

Yalei Wang,^{a,b} Jun Song,^{*, b} and Wai-Yeung Wong^{*, a,c}

Supporting Figures

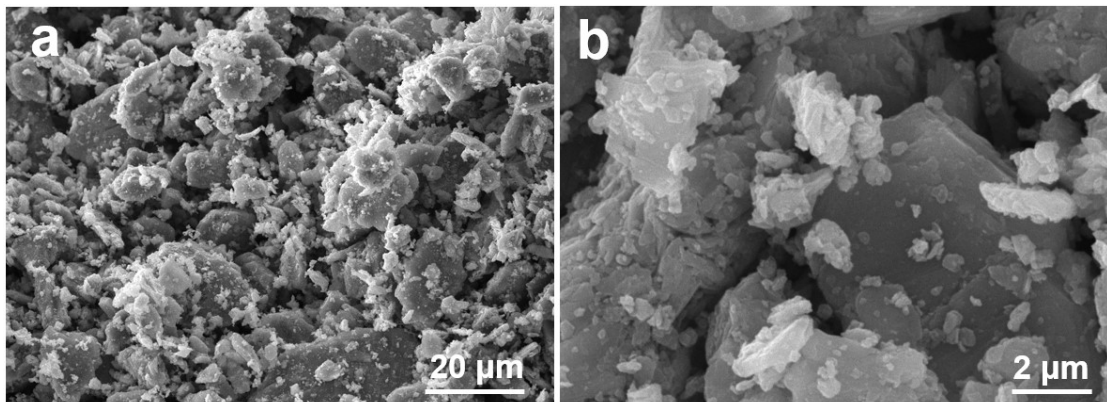


Fig. S1. SEM images of the Ti_3AlC_2 MAX phase.

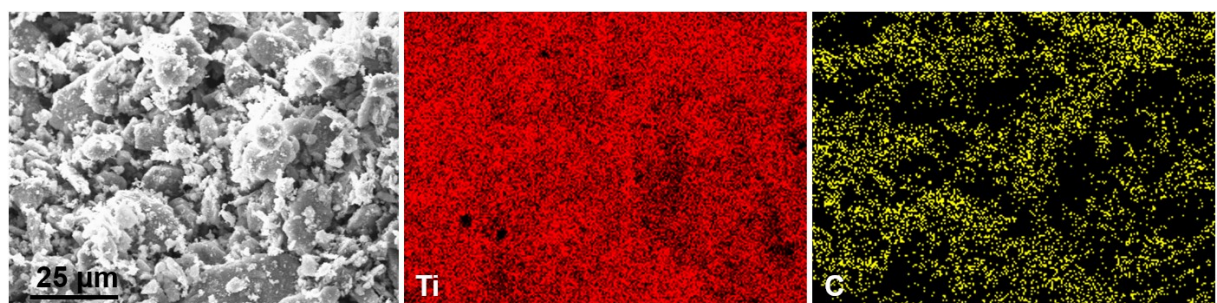


Fig. S2. Mapping images of the Ti_3AlC_2 MAX phase.

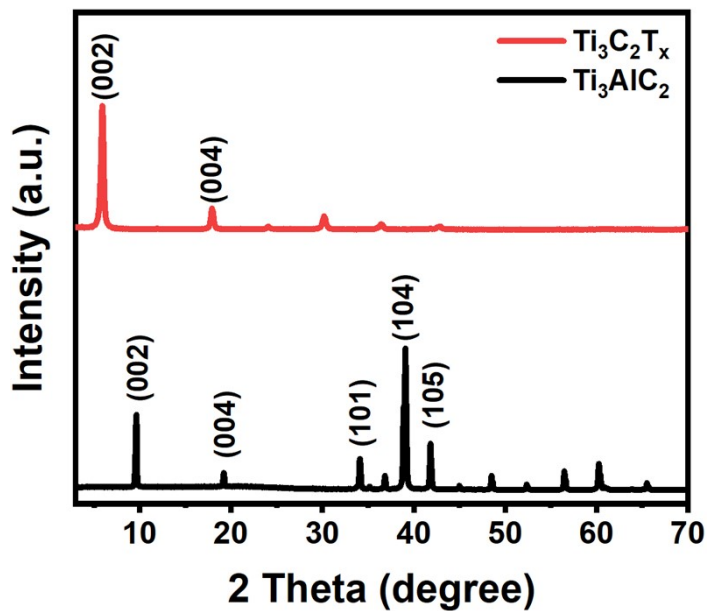


Fig. S3. XRD patterns of the Ti_3AlC_2 MAX and $\text{Ti}_3\text{C}_2\text{T}_x$.

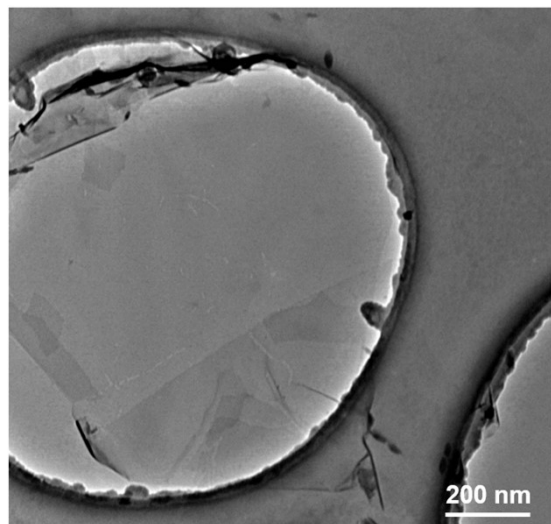


Fig. S4. TEM images of the $\text{Ti}_3\text{C}_2\text{T}_x$ nanosheets.

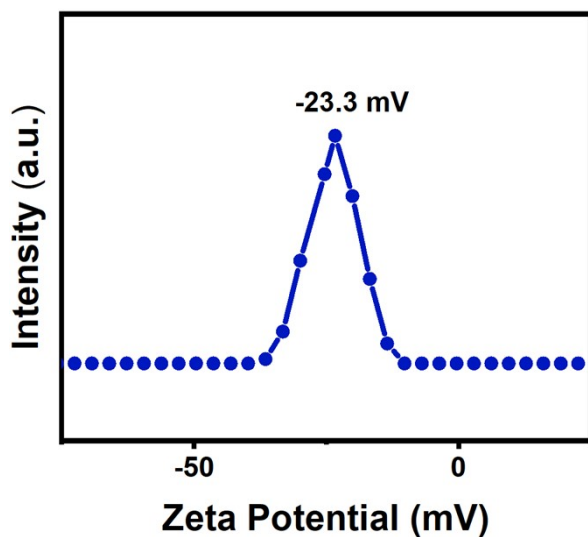


Fig. S5. Zeta potentials of the $\text{Ti}_3\text{C}_2\text{T}_x$ MXene solution.

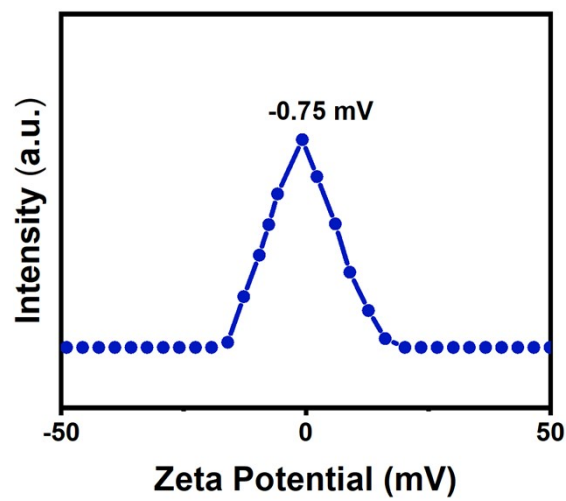


Fig. S6. Zeta potentials of the PANI/MXene solution.

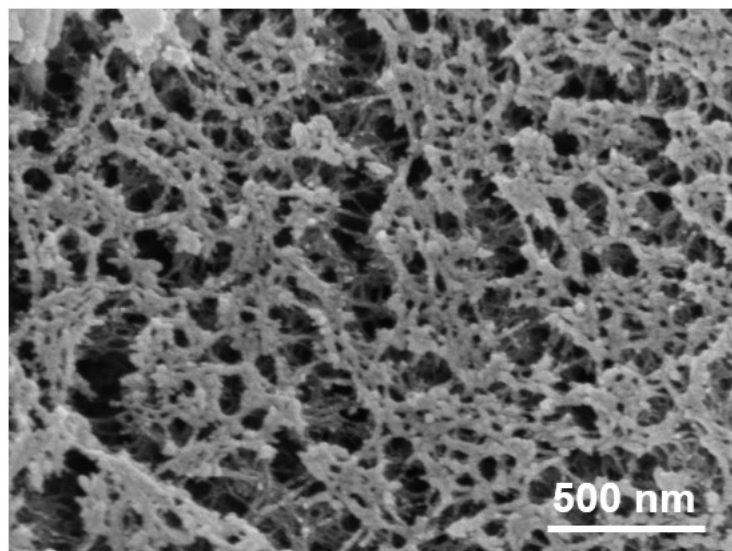


Fig. S7. SEM images of the PANI/MXene.

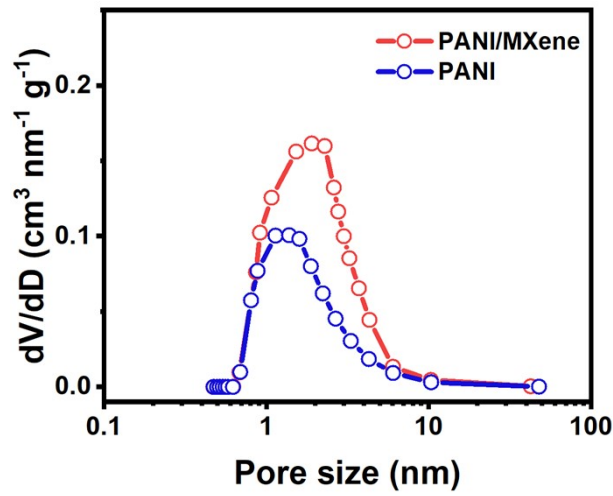


Fig. S8. The pore size distribution of the PANI/MXene and PANI cathode.

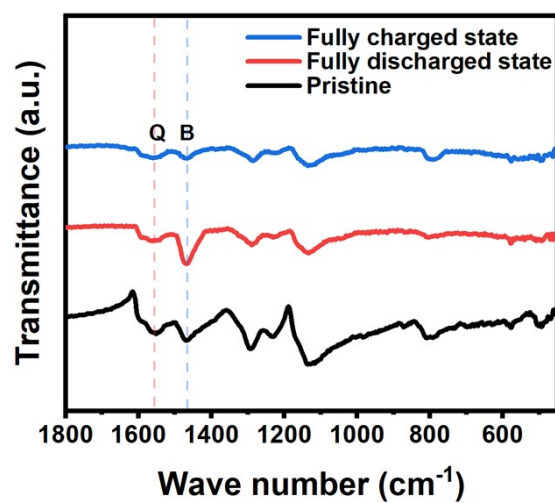


Fig. S9. The FTIR spectra in pristine, fully discharged, and fully charged states.

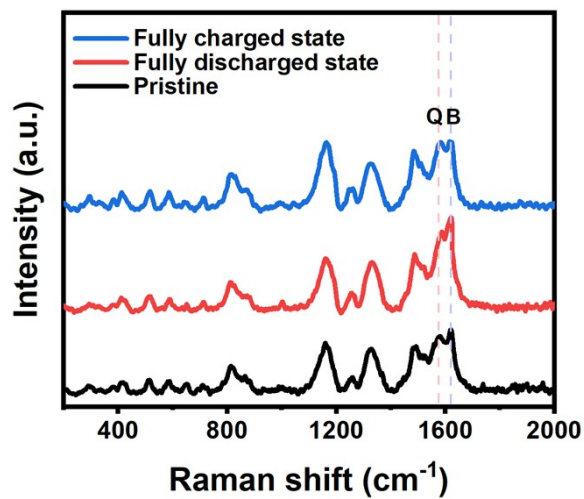


Fig. S10. The Raman spectra in pristine, fully discharged, and fully charged states.

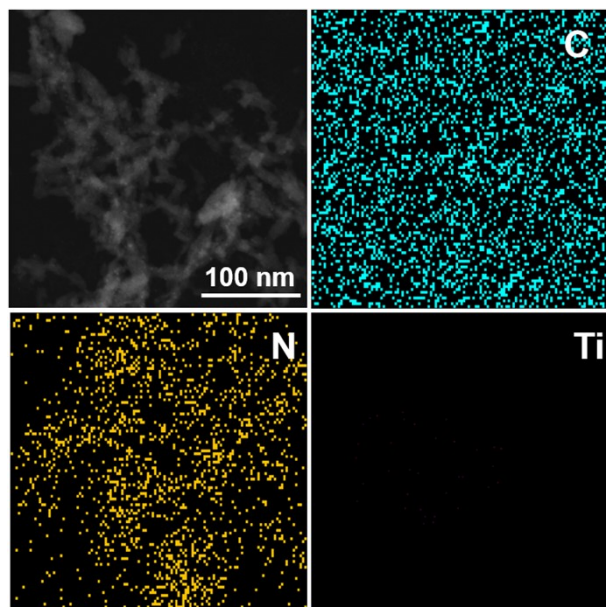


Fig. S11. STEM and the corresponding elemental mapping images of the PANI.

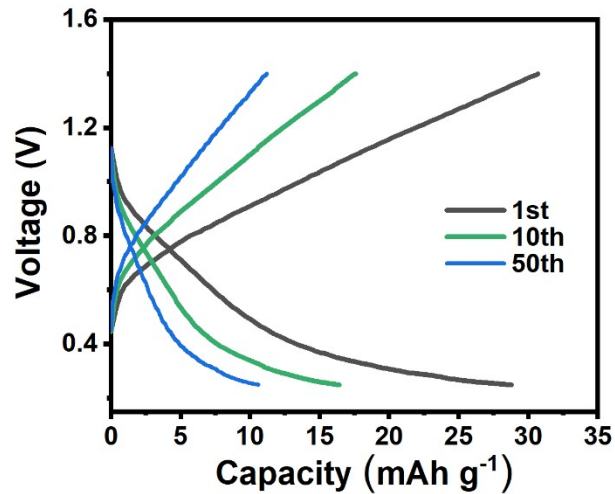


Fig. S12. Charge/discharge curves of MXene nanosheets at 0.2 A g^{-1} .

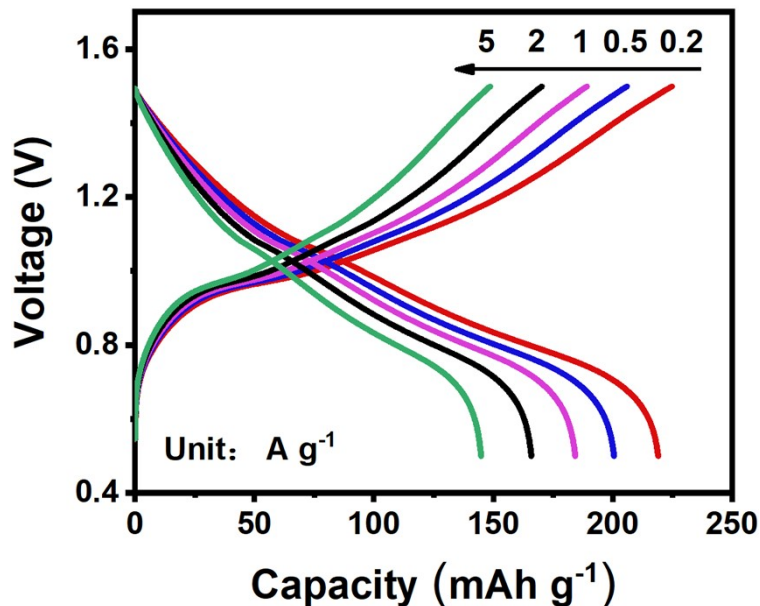


Fig. S13. Charge/discharge curves of the PANI/MXene at different current densities.

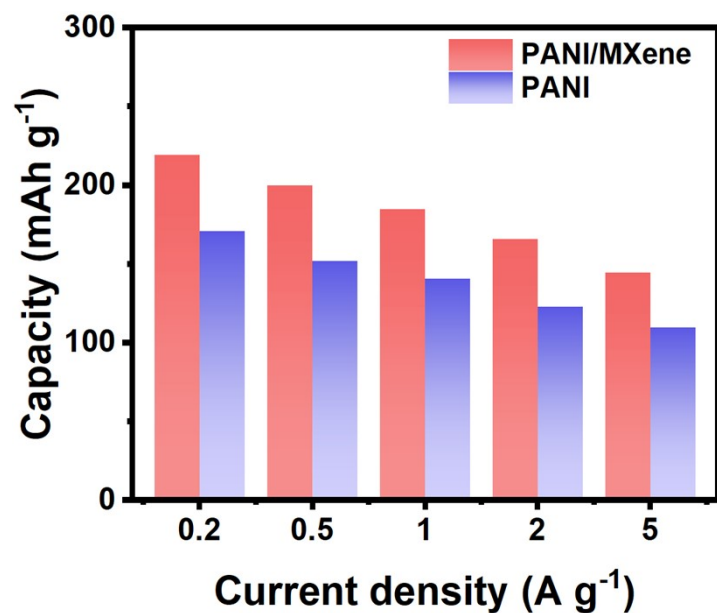


Fig. S14. The average capacities of the PANI/MXene and PANI.

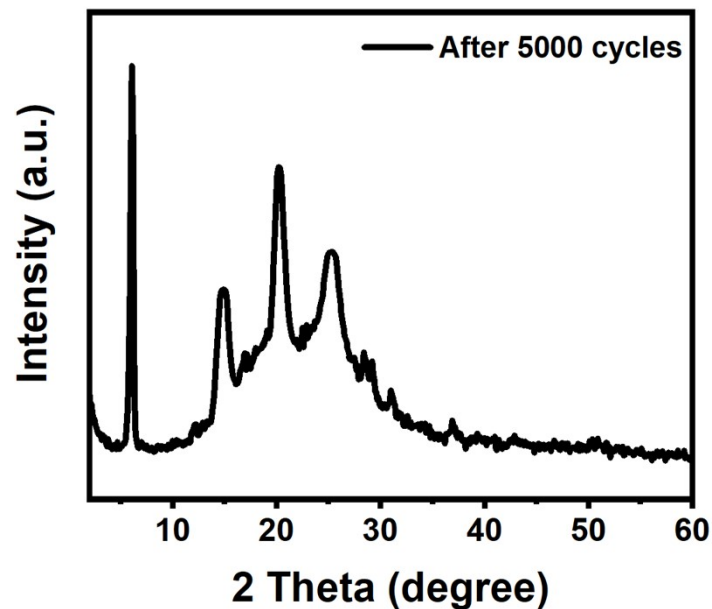


Fig. S15. The XRD pattern of the PANI/MXene after 5000 cycles.

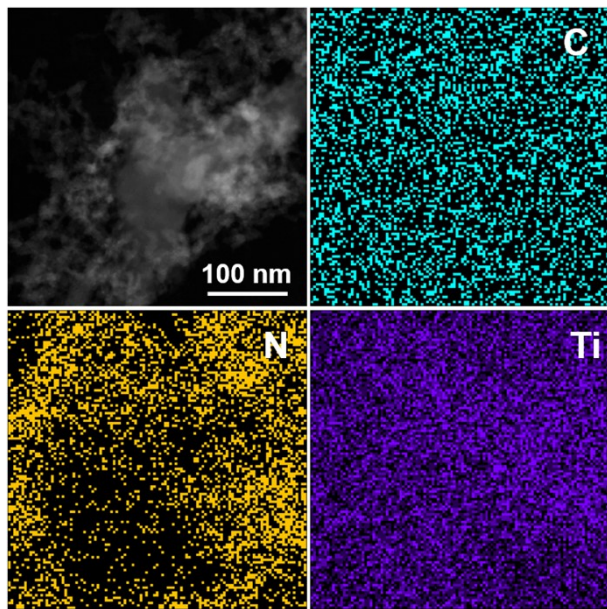


Fig. S16. STEM and the corresponding elemental mapping images of the PANI/MXene after 5000 cycles.

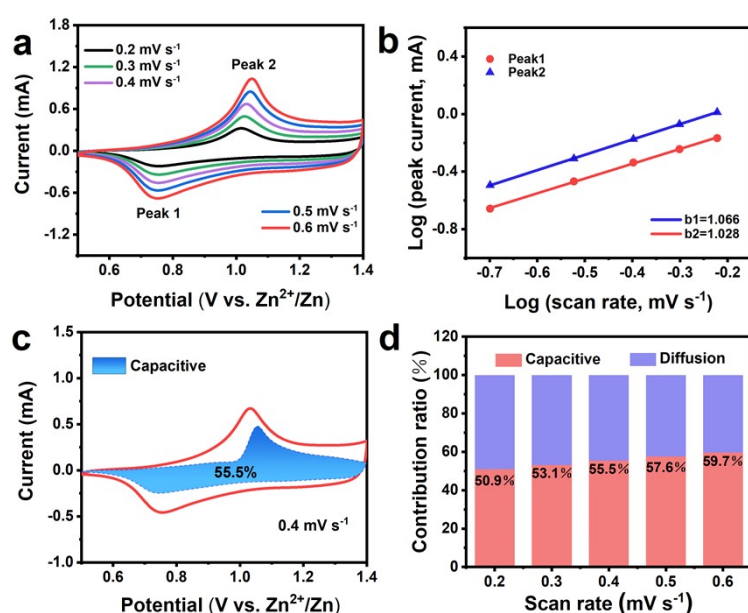


Fig. S17 The electrochemical kinetics of the PANI cathode. a) CV curves at various scan rates. b) $\log v$ vs. $\log i$ plots according to the CV curves. c) The CV curve with a capacitive contribution at 0.4 mV s^{-1} . d) The capacitive contribution ratios at various scan rates.

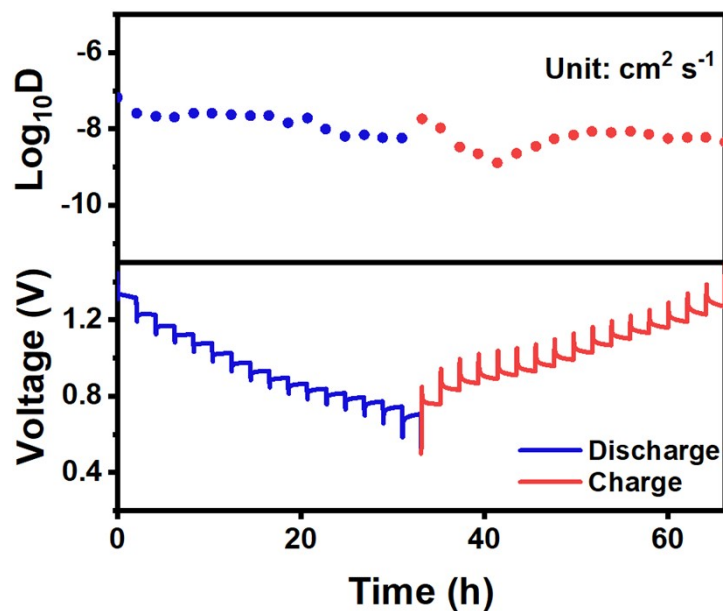


Fig. S18. GITT curves of the PANI/MXene and the corresponding ion diffusion coefficients.

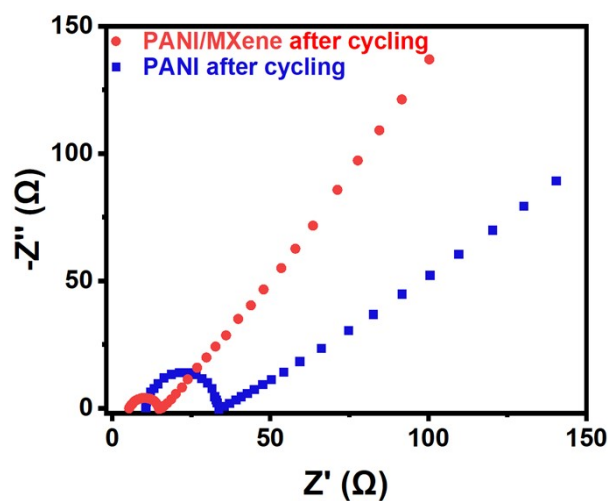


Fig. S19. Nyquist plots of the PANI/MXene and PANI after 5000 cycles.

Table S1. Comparisons of the electrochemical performance of PANI/MXene with other PANI-based electrodes.

Cathode material	Mass loading (mg cm ⁻²)	Capacity (mAh/g)	Capacity retention (%)	Ref.
PANI/MXene	1.5	147.4 (5 A/g)	88.3 % (5000 cycles)	This work
PANI/carbon felts	1.5	89.1 (5 A/g)	92.0 % (3000 cycles)	[S1]
PANI-S	1.2	130.1 (10 A/g)	84.6 % (2000 cycles)	[S2]
PANI/SWCNTs film	1.5	135.8 (1 A/g)	97.3 % (1000 cycles)	[S3]
PANI-SWCNT-sponge	3.0	115 (1 A/g)	94.0 % (500 cycles)	[S4]
OCF/PANI	2.4	119.4 (0.1 A/g)	95.4 % (200 cycles)	[S5]
PANI@CNT	—	107.6 (0.5 A/g)	91.1 % (150 cycles)	[S6]
ZnHCF/PANI	1.5	85.0 (0.5 A/g)	75.0 % (350 cycles)	[S7]
KCY@PANI	0.83	141.9 (2 A/g)	88.0 % (2000 cycles)	[S8]

[S1] F. Wan, L. Zhang, X. Wang, S. Bi, Z. Niu and J. Chen, *Adv. Funct. Mater.*, 2018, **28**, 1804975.

[S2] H. Y. Shi, Y. J. Ye, K. Liu, Y. Song and X. Sun, *Angew. Chem. Int. Ed.*, 2018, **57**, 16359-16363.

[S3] M. Yao, Z. Yuan, S. Li, T. He, R. Wang, M. Yuan and Z. Niu, *Adv. Mater.*, 2021, **33**, 2008140.

[S4] H. Cao, F. Wan, L. Zhang, X. Dai, S. Huang, L. Liu and Z. Niu, *J. Mater. Chem. A*, 2019, **7**, 11734-11741.

[S5] H. Yu, G. Liu, M. Wang, R. Ren, G. Shim, J. Y. Kim, M. X. Tran, D. Byun and J. K. Lee, *ACS Appl Mater Interfaces*, 2020, **12**, 5820-5830.

[S6] X. Xiao, W. Liu, K. Wang, C. Li, X. Sun, X. Zhang, W. Liu and Y. Ma, *Nanoscale Adv.*, 2020, **2**, 296-303.

[S7] Q. Liu, Z. Ma, Z. Chen, M. Cui, H. Lei, J. Wang, J. Fei, N. He, Y. Liu, Q. Liu, W. Li and Y. Huang, *Chem. Commun.*, 2022, **58**, 8226-8229.

[S8] G. Shim, M. X. Tran, G. Liu, D. Byun and J. K. Lee, *Energy Storage Mater.*, 2021, **35**, 739-749.